Structure of photon

S. Söldner-Rembold
M. Wing
M. Krawczyk

Inclusive production of

- jets
- prompt photons
- heavy quarks (c/b)

in a <u>real γ</u> proton int.

in a <u>virtual γ</u> proton int.

transverse (long.?)

Goals → partonic structure of γ and γ^*

QCD predictions for γ

for γ^* ← unique test of QCD (Witten, Rossi ....)

Exclusive photoproduction

$\gamma p \to V p$ $\gamma p \to a p$ $a - \pi^0, \eta, \eta' \ldots$

Thanks to

J. Butterworth
M. Wing
S. Söldner-Rembold
A. de Roeck
P. Janhorski
A. Zembrushi
V. Jezuita-Dąbrarska
P. Landshoff
I. Ginzburg
F. Canet
B. Levtchenko
J. Crittenden
J. Chyla
...

Photon - a gauge boson of QED

1900 - Planck - quanta of energy

1905 - Einstein hipothesis - quanta of light

⋮

Presently main information on the strong (hadronic,partonic) properties of :

→ real photon γ

→ virtual photon γ^*

comes from

"How photon structure is measured ?
- With great difficulty."
J.M. Butterworth '99

Deep Inelastic Scattering on a photon in the e^+e^- collisions

Growing importance of the measurements of resolved photon processes in e^+e^- and ep collisions.

Last two years -

spotlight on a virtual photon!

S. Soldner-Rembold

parton parametrisations F_2 for real γ

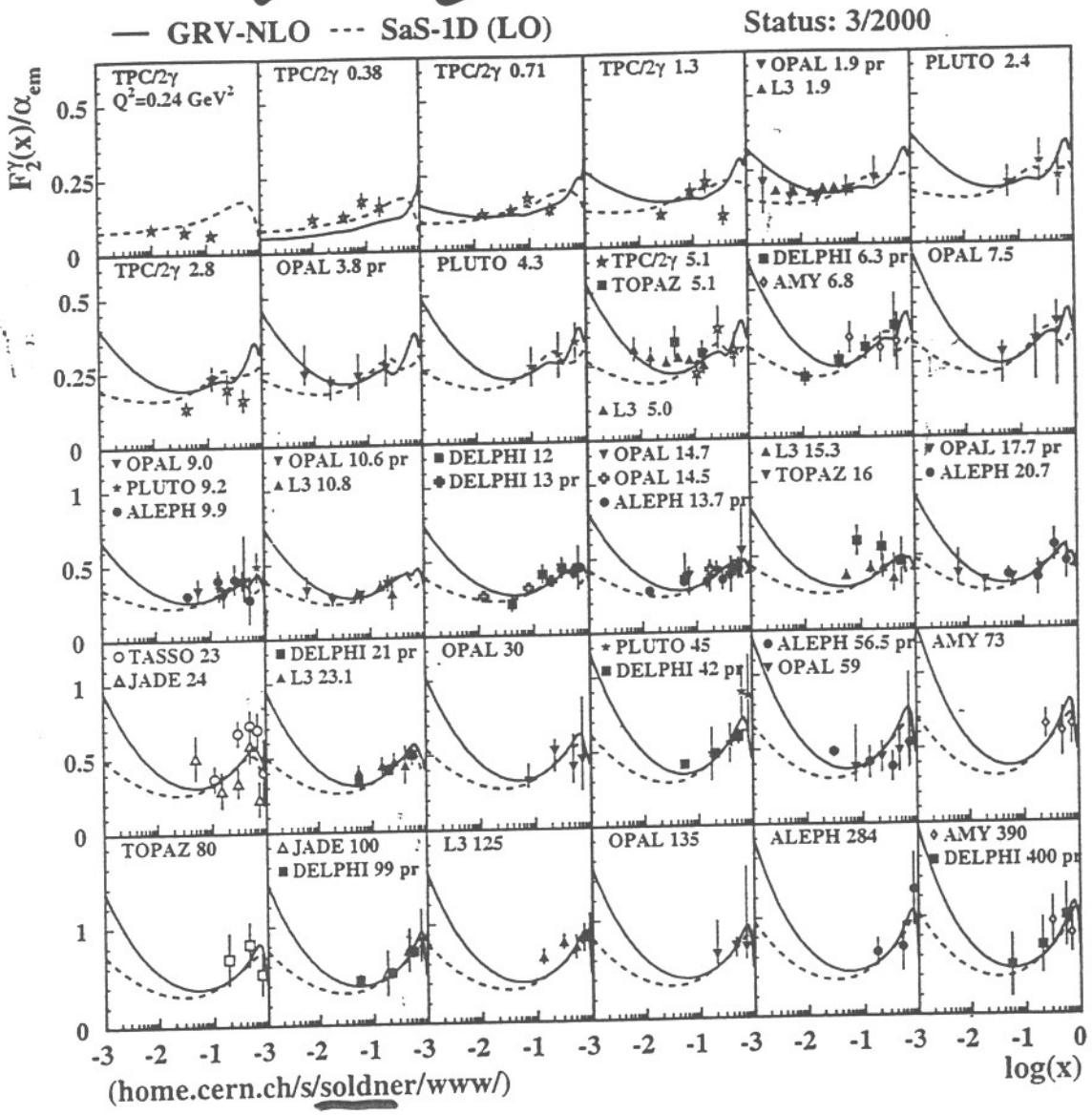

(home.cern.ch/s/soldner/www/)

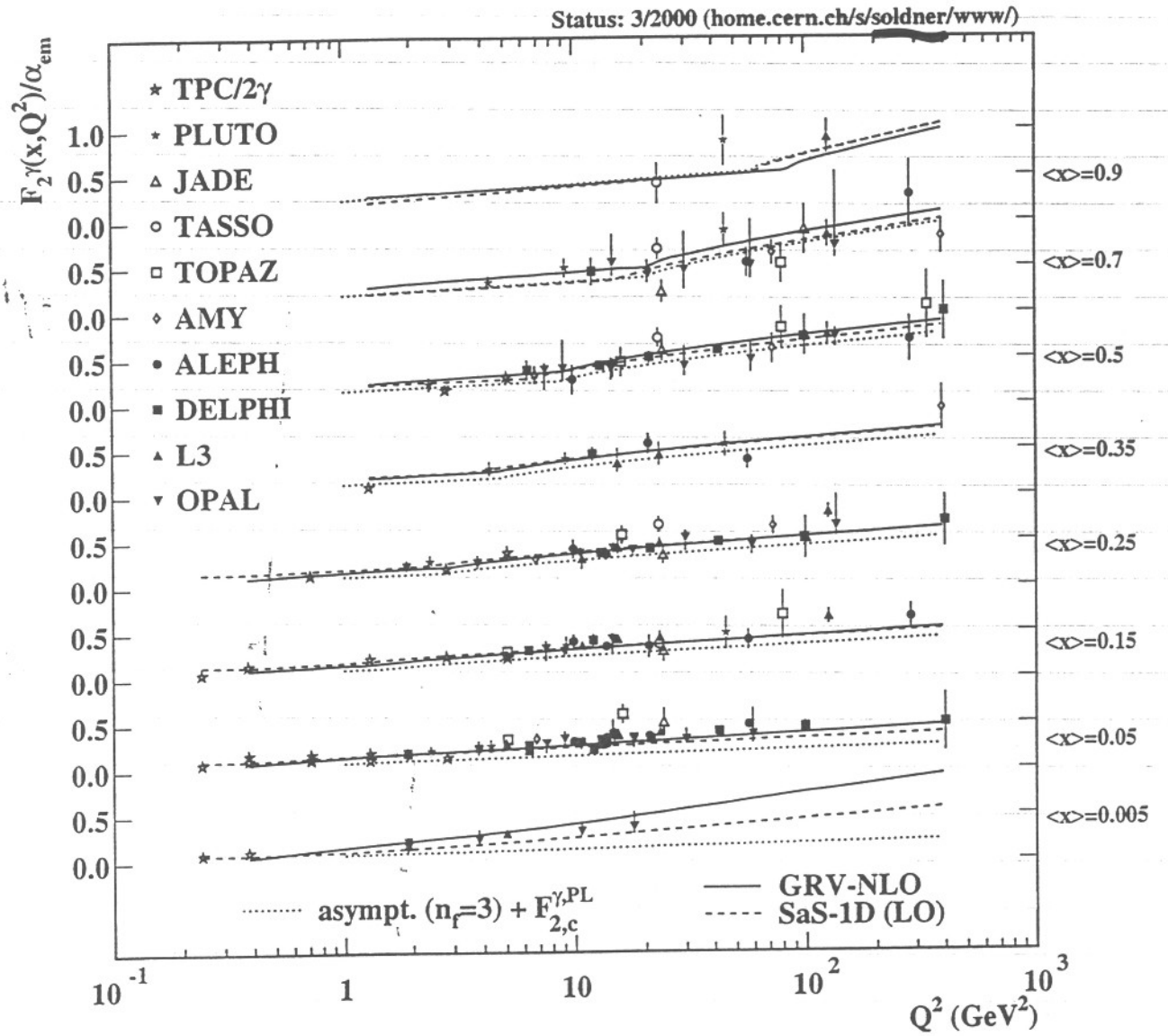
Status: 3/2000 (home.cern.ch/s/soldner/www/)
$F_2^\gamma(x,Q^2)/\alpha_{em}$
TPC/2γ
PLUTO
JADE
TASSO
TOPAZ
AMY
ALEPH
DELPHI
L3
OPAL
<x>=0.9
<x>=0.7
<x>=0.5
<x>=0.35
<x>=0.25
<x>=0.15
<x>=0.05
<x>=0.005
asympt. (n_f=3) + $F_{2,c}^{\gamma,PL}$
GRV-NLO
SaS-1D (LO)
Q^2 (GeV^2)

from K. Miller
Jerusalem '97

(dijets)

HERA

scaling violation

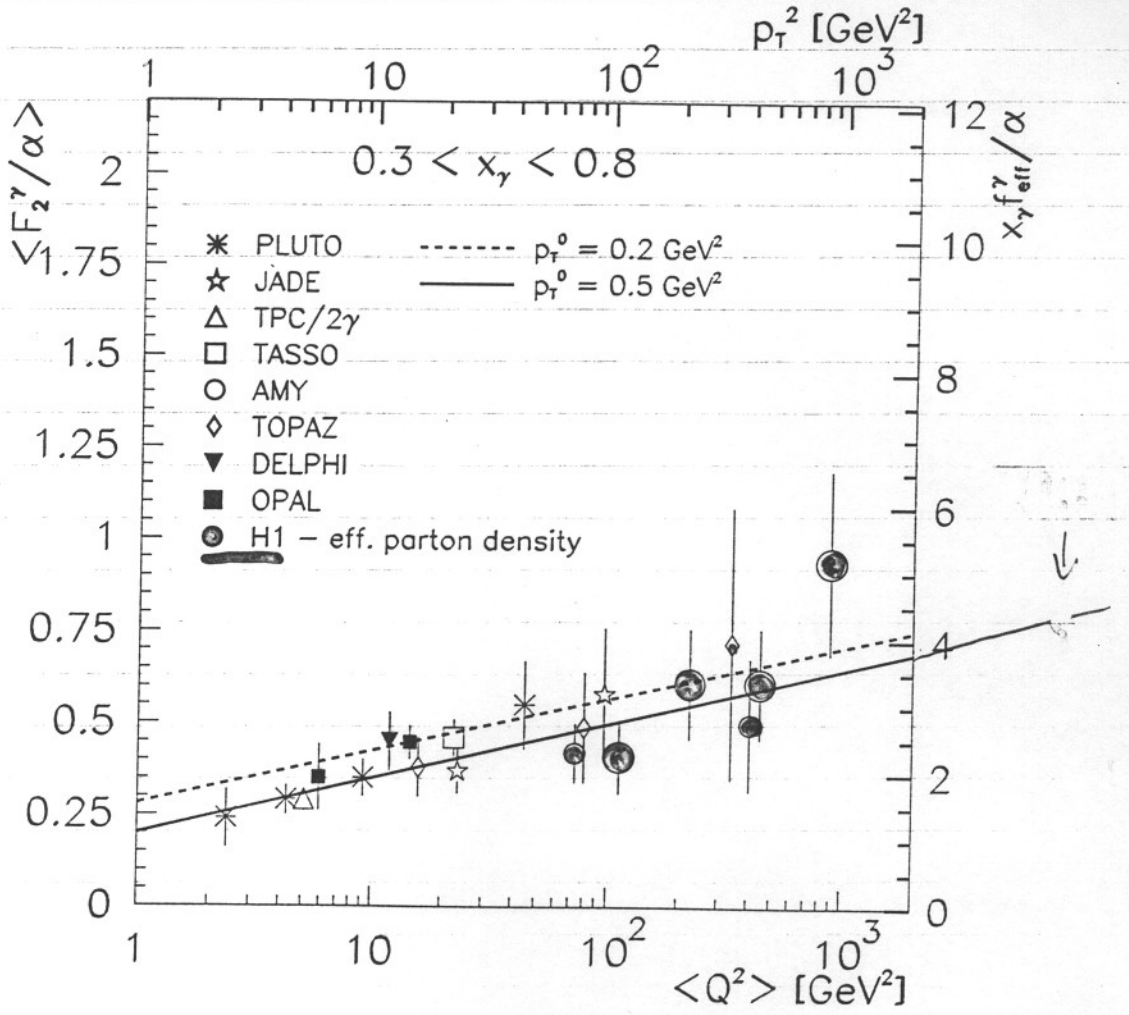

Is a new parametrization for real photon PDF needed?

F. Cornet
Univ. of Granada

Discrepancies observed in present data:

* Dijet production
* Prompt photon
* Heavy flavor production

$x_p \sim 10^{-2} - 10^{-1}$ well known

$x_\gamma \sim 0.1 - 1$

$E_T^{leading} > 14$ GeV

$E_T^{second} > 11$ GeV

$\int L\,dt = 6.3\,pb^{-1}$

8690 events

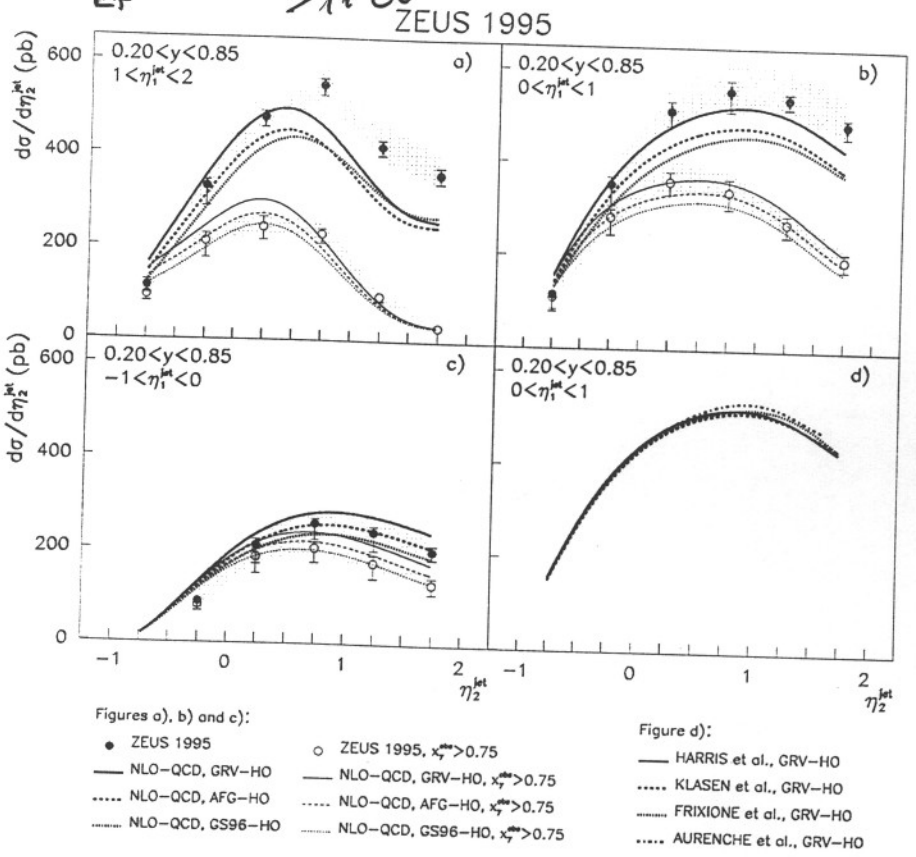

Figure 5: Figures a), b) and c) show the dijet cross section as a function of η_2^{jet} in bins of η_1^{jet}. The filled circles correspond to the entire x_γ^{obs} range while the open circles correspond to events with $x_\gamma^{obs} > 0.75$. The shaded band indicates the uncertainty related to the energy scale. The thick error bar indicates the statistical uncertainty and the thin error bar indicates the systematic and statistical uncertainties added in quadrature. The full, dotted and dashed curves correspond to NLO-QCD calculations, using the GRV-HO, GS96-HO and the AFG-HO parameterisations for the photon structure, respectively. In d) the NLO-QCD results for the cross section when $0 < \eta_1^{jet} < 1$ and for a particular parameterisation of the photon structure are compared.

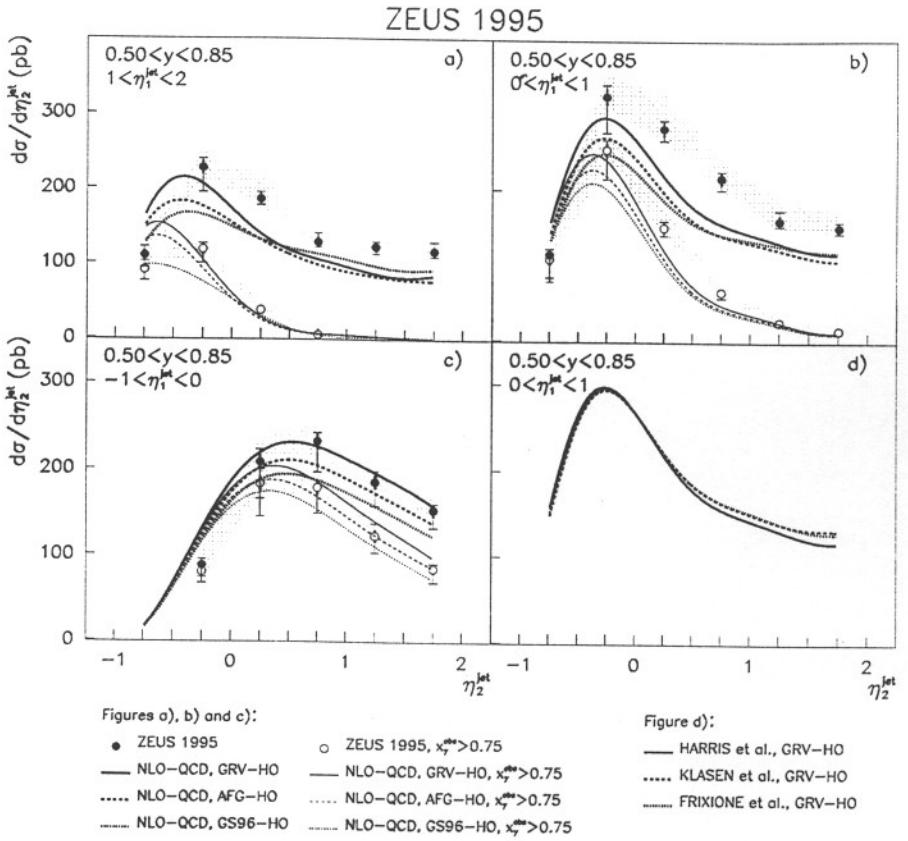

Figure 6: Figures a), b) and c) show the dijet cross section as a function of η_2^{jet} in bins of η_1^{jet} and for $0.50 < y < 0.85$. The filled circles correspond to the entire x_γ^{obs} range while the open circles correspond to events with $x_\gamma^{obs} > 0.75$. The shaded band indicates the uncertainty related to the energy scale. The thick error bar indicates the statistical uncertainty and the thin error bar indicates the systematic and statistical uncertainties added in quadrature. The full, dotted and dashed curves correspond to NLO-QCD calculations, using the GRV-HO, GS96-HO and the AFG-HO parameterisations for the photon structure, respectively. In d) the NLO-QCD results for the cross section when $0 < \eta_1^{jet} < 1$ and for a particular parameterisation of the photon structure are compared.

Lower ambiguity due to hadronization

$E_T^\gamma > 5$ GeV

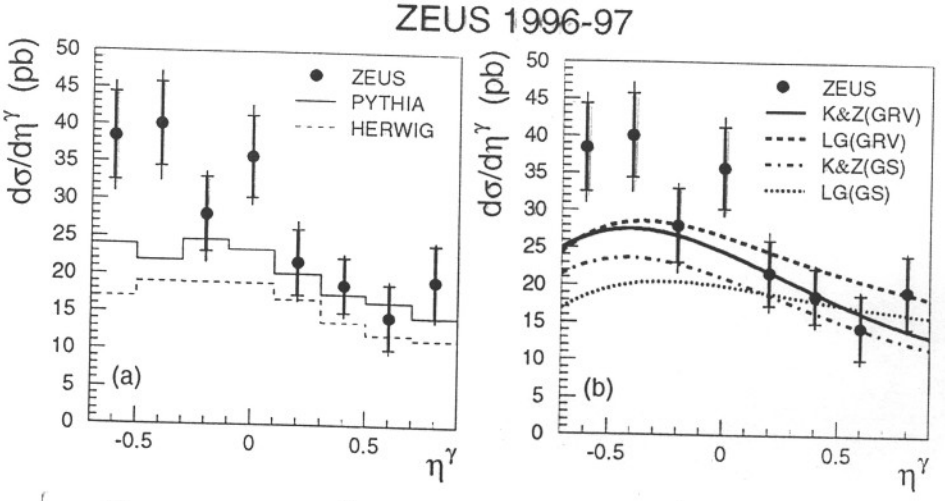

$\int L\,dt = 38.4\ pb^{-1}$ → 6000 events

Figure 3: Differential cross-section $d\sigma/d\eta^\gamma$ for isolated prompt photons with $5 < E_T^\gamma < 10$ GeV, for $0.2 < y < 0.9$ ($134 < W < 285$ GeV). The inner (thick) error bars are statistical; the outer include systematic errors added in quadrature. Also plotted are (a) PYTHIA and HERWIG predictions using the GRV(LO) photon parton densities; (b) LG and K&Z NLO predictions using GRV(HO) and GS(HO) photon parton densities.

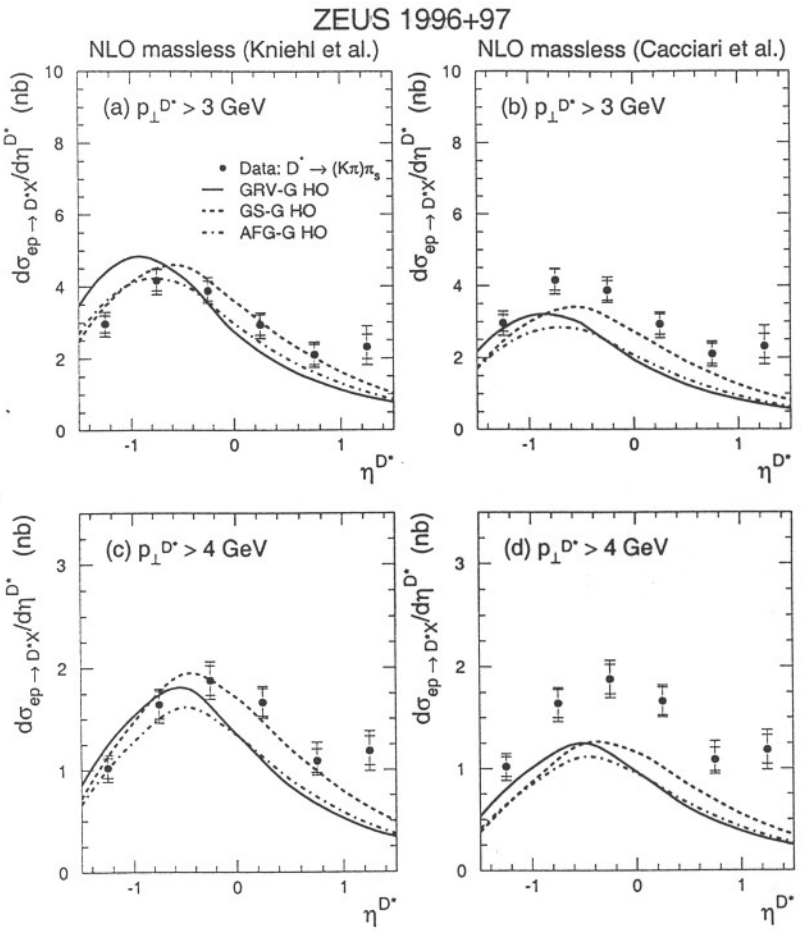

Fig. 4. Differential cross sections $d\sigma/d\eta^{D^*}$ for D^* photoproduction, $Q^2 < 1\,\mathrm{GeV}^2$, in the kinematic region $130 < W < 280\,\mathrm{GeV}$ for the $(K\pi)\pi_S$ channel with **a**, **b** $p_T^{D^*} > 3\,\mathrm{GeV}$ and **c**, **d** $p_T^{D^*} > 4\,\mathrm{GeV}$. The points are drawn at the centres of the corresponding bins. The inner part of the error bars shows the statistical error, while the outer one shows the statistical and systematic errors added in quadrature. The curves are the predictions of the massless charm NLO of [6] **a**, **c** and [8] **b**, **d** with various photon parton density parametrisations

in Table 1 and shown as full lines in Figs. 2 and 3. The parton density parametrisations used were CTEQ4M [37] for the proton and GRV-G HO [27] for the photon. The renormalisation and factorisation scales as well as the values of m_c are the same as in the calculation of the massive charm approach.

The predictions of the two massless charm models give similar shapes of the differential cross sections (Figs. 2 and 3), but disagree with each other in absolute magnitude by $\simeq$ 40%. The cross sections obtained by these predictions are mostly below the data. In particular the data are above the NLO expectations in the forward direction. The contribution of D^* produced from $b\bar{b}$ in our kinematic region, not included in the NLO curves, is predicted [5] to be below 5%, in agreement with our MC estimation (Sect. 4). This fraction is found from the MC studies to be slightly higher in the forward region, where it is up to 7%.

Using the MRSG [26] parton density parametrisation of the proton has no significant effect on the predictions. In contrast, the calculations depend on the parton density parametrisations of the photon and in particular its charm content. In order to check the sensitivity of the $d\sigma/d\eta^{D^*}$ data to the parton density parametrisation of the photon, we compare the results for $p_T^{D^*} > 3\,\mathrm{GeV}$ and $p_T^{D^*} > 4\,\mathrm{GeV}$ in Fig. 4 with the two NLO massless charm predictions [6, 8] obtained with the photon parton density parametrisations GRV-G HO [27], GS-G HO [38] and AFG [39]. The differences between the various photon parton densities are at the 20% level or less in the integrated cross sections, but in the differential cross sections considerable differences in shape are observed. For the massless charm scheme of [6], the GS-G HO curves [38] are closest to the data. However, in the GS-G HO parton density function used for this calculation, charm and u-quarks contribute equally.

7 Measurement of D^* dijet cross sections

Given the discrepancies observed between data and NLO predictions in the inclusive D^* measurements, it is of interest to study the kinematics of charm production in more detail. The measurement of jets in the final state allows the kinematics of the hard scattering process to be recon-

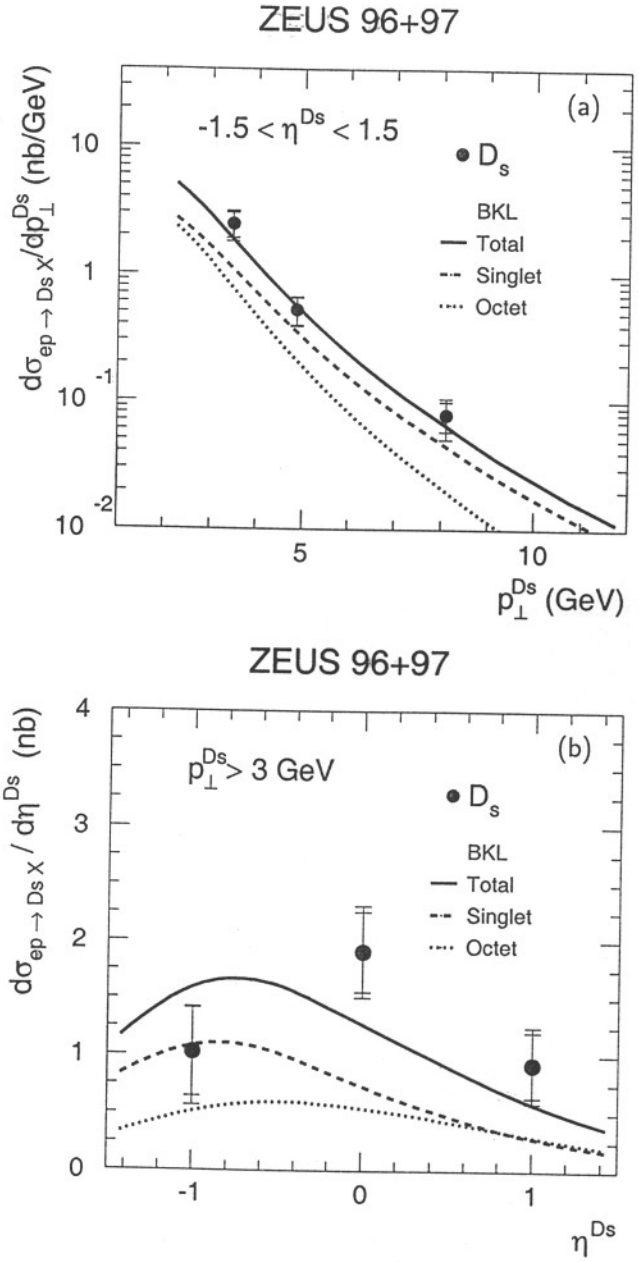

Figure 3: Differential cross sections for the photoproduction reaction $ep \to D_s X$: (a) $d\sigma/dp_\perp^{D_s}$ and (b) $d\sigma/d\eta^{D_s}$ compared to the BKL model [6]. Colour-singlet (dashed curves) and colour-octet (dotted curves) contributions are plotted separately. Their sum is shown as the full curves. The $p_\perp^{D_s}$ points are drawn at the position of the average value of an exponential fit in each bin. The η^{D_s} points are drawn at the middle of each bin. The inner error bars show the statistical uncertainty, while the outer ones show the statistical and systematic errors added in quadrature. Normalisation uncertainties due to the $D_s \to \phi\pi$ branching ratio are not included in the systematic errors or in the theoretical calculations.

H1 $\sigma(\gamma p \to b\bar{b}X) = 111 \pm 10 \,^{+43}_{-20}$ nb

$= 63$ nb (Frixione et al.)

THERA

F_2^γ at LEP I and LEP II

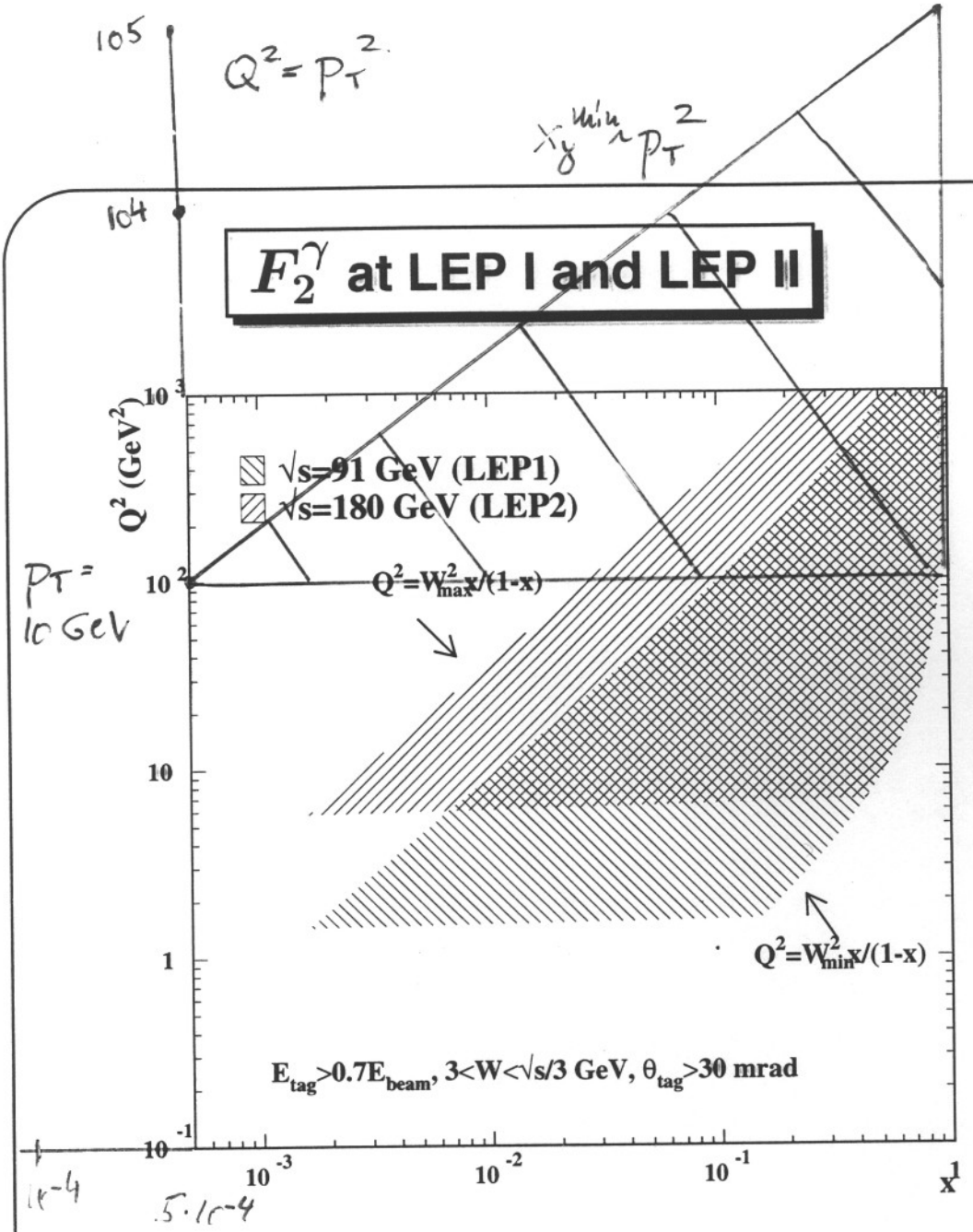

$$Q^2 \approx 2E_{\mathrm{beam}}E_{\mathrm{tag}}(1-\cos\Theta_{\mathrm{tag}})$$

Identical Q^2 ranges can be covered with different detectors at LEP1 and LEP2

Resolved γ processes

- jets → M. Wing, J. Butterworth
- prompt photons → A. Zembrzuski, MK
- heavy quarks → M. Wing, J. Butterworth
  P. Jankowski, MK
  A. de Roeck

  → L. Gladilin

M. Wing, J. Br

Current Situation at HERA, $\sqrt{s} = 318$ GeV

Where are the resolved photon processes?

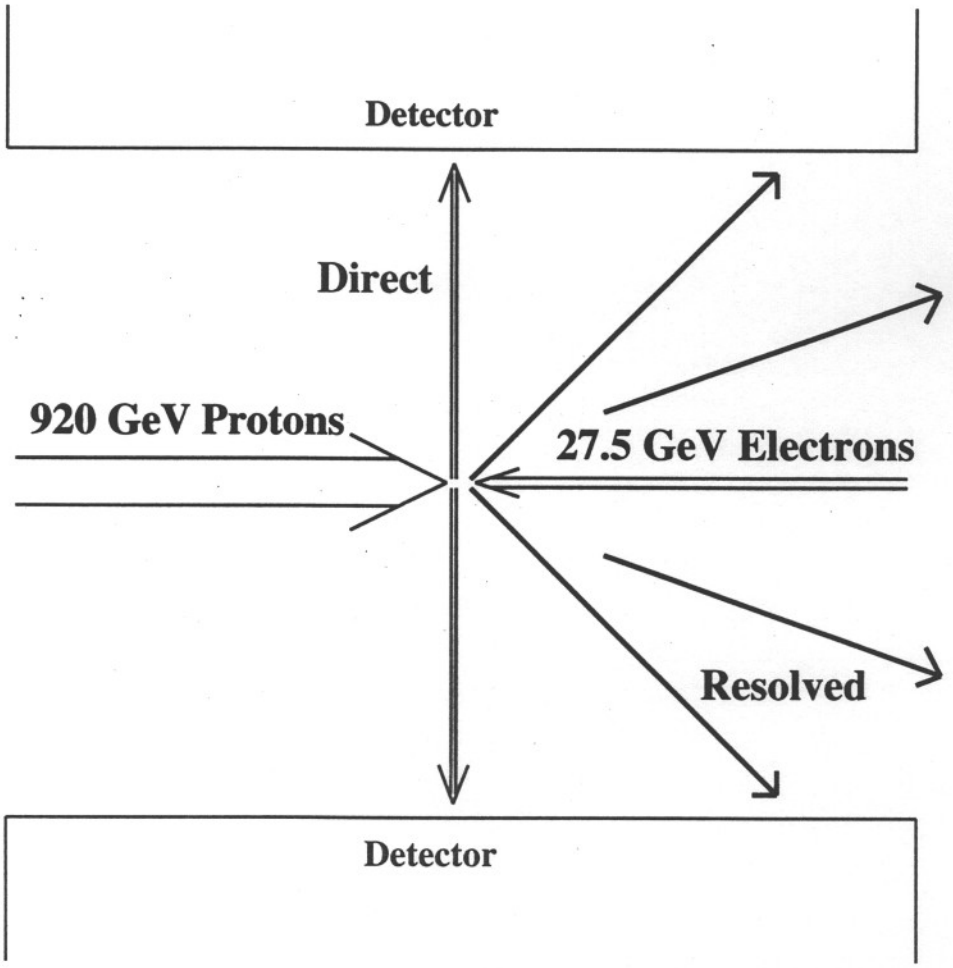

Due to large asymmetry in beam energies:

- Direct photon processes are centralised.
- Resolved photon processes in forward parts of the detector.
- Resolved processes have a large cross-section, but alot is lost in the forward region.

Potential Situation at TERA,

$$\sqrt{s} = 959 \text{ GeV}$$

Where are the resolved photon processes?

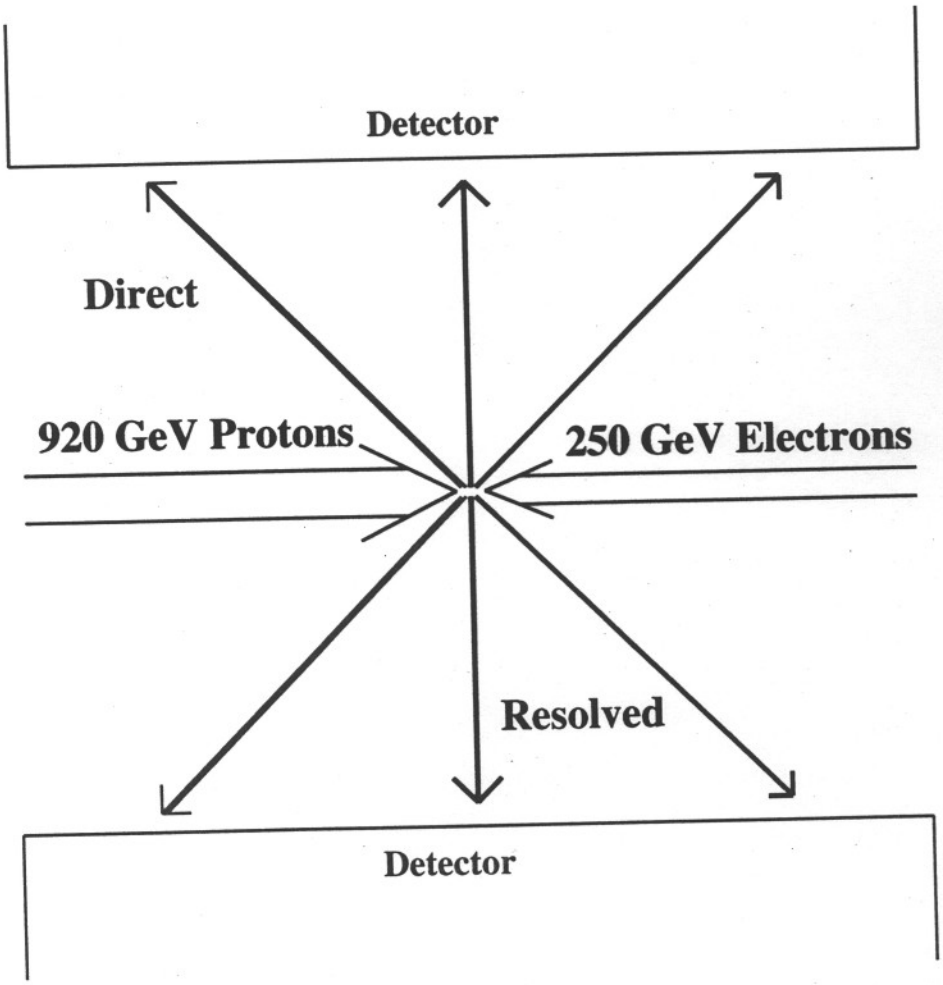

Due to reduced asymmetry in beam energies:

- Direct photon processes are more in rear part of detector.
- Resolved photon processes in *central* and forward parts of the detector.

Cross-Sections in η^{jet}

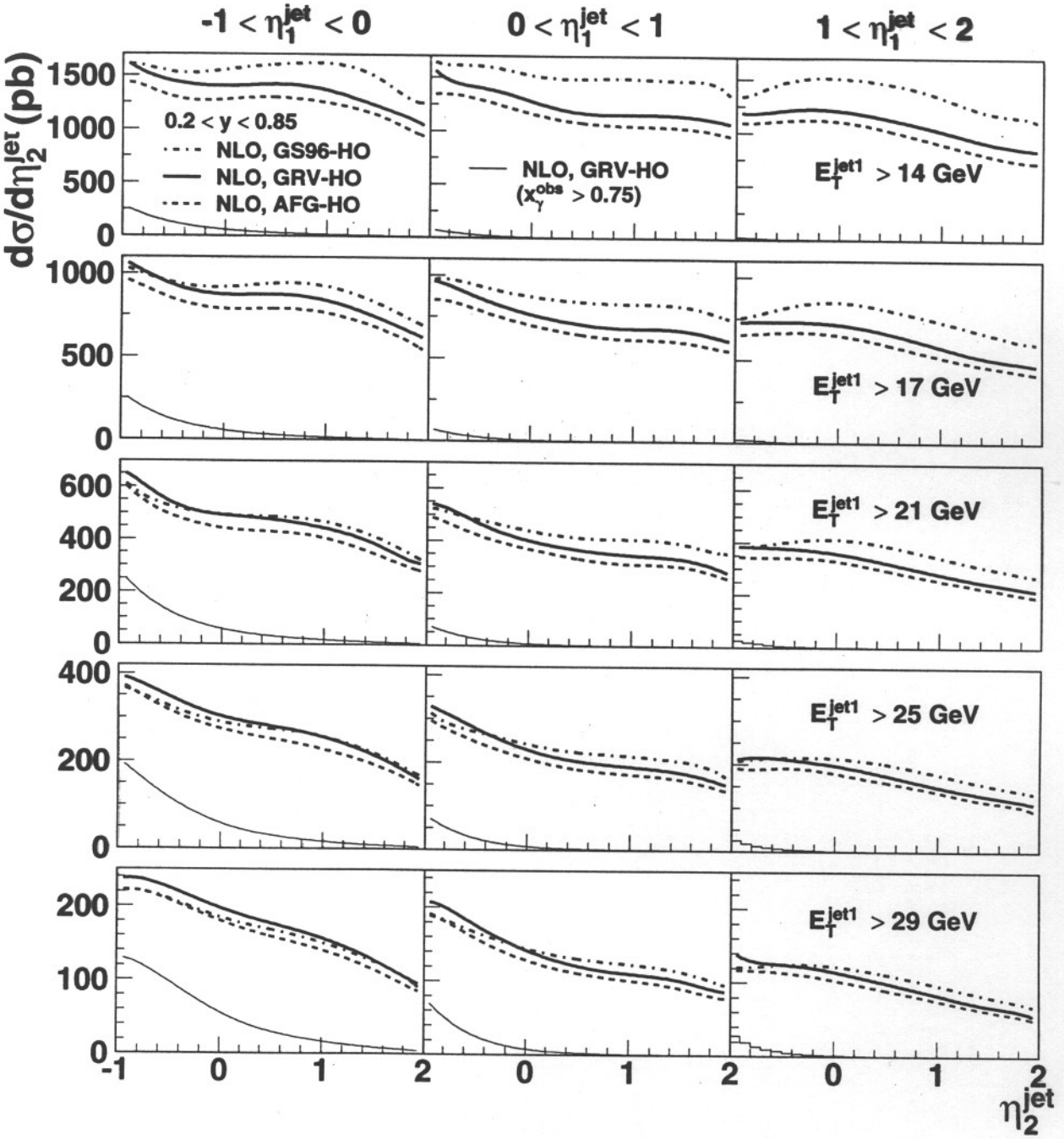

At lower E_T^{jet1}:

- Prediction with GS96-HO is significantly larger.
- Almost all cross-section is from the resolved photon.

Magnitude of Differences

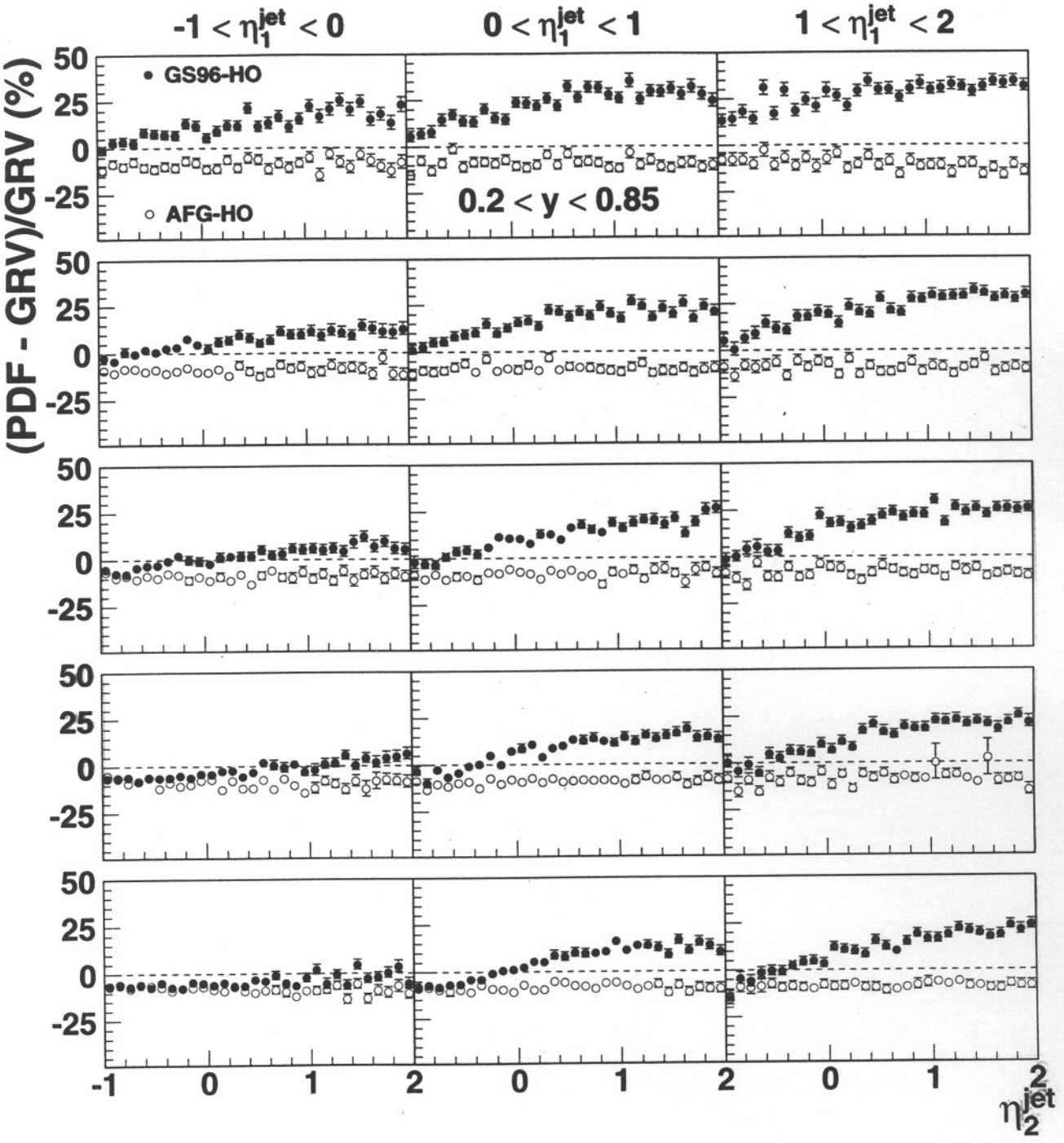

Cross-sections sensitive to choice of PDF; up to 35%!

Conclusions and Outlook

- Promising first look shown.
  - Studied high E_T^{jet} production and a quick look at charm.
- Both NLO and MC predictions show sensitivity to choice of photon PDF.
- Differences between PDFs up to 35%.
- Plan to work on differenes between NLO calculations (M. Klasen).
- More MC data needed with more structure functions.
- Other ideas... ?

M. Krawczyk
A. Zembrzuski
NLO calculation

Prompt photons at THERA

$ep \to e\gamma X$
photoproduction $Q^2 \approx 0$

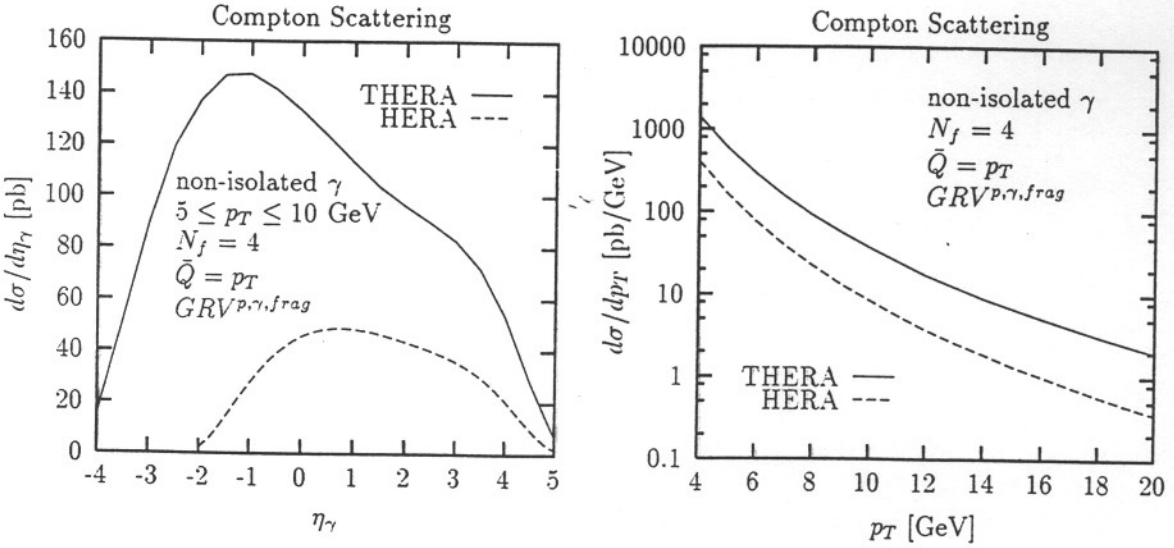

$0 < y = E_\gamma/E_e < 1$
$Q^2 \leq 1\ \mathrm{GeV}^2$

dominated by $q^{\gamma} q \to \gamma q$ process → probing q^{γ}

similar picture for virtual-γp via $\gamma^* p \to \gamma X$ → probing q^{γ^*}!

Heavy quark production

→ L. G. talk

- sensitive to parton density in γ (forward direction)
- comparison to L.C & PC

Parton parametrizations for the virtual photon

The notion of the partonic content of the virtual photon ($P^2 \neq 0$) can be applied if Q^2 scale is larger than P^2 (typically $P^2 \lesssim 0.2\ Q^2$).

The parton distributions in the virtual photon can (?) be calculated in the perturbative QCD for $\Lambda^2 \ll P^2 \ll Q^2$ without any input, for lower P^2 extra assumptions are needed.

γ^*_T
- Drees - Godbole
- Glück - Reya - Stratmann (GRS)
- Schuler - Sjöstrand (SaS)
- Glück - Reya - Schienbein (GRSch)
- Gorski - Ioffe - Khodjamirian - Oganesian (GIKO)
- Ioffe - Oganesian (IO)
- Chýla

γ^*_L

Resolved γ^* processes

- jets → B. Pötter → MC
  U. Jezuita-Dąbrowska
- prompt photons → A. Zembrzuski, MK
  U. Jezuita-Dąbrowska
- heavy quarks → M. Wing, J. Butterworth
  P. Jankowski, MK
  A. de Roeck,
  – in preparation
  ⋮

---

transverse γ^*

longitudinal γ^* ?

Prompt photon production in $\gamma^* p$ collision

γ_T^* content

$g^{\gamma^*} q^p \to \gamma q$

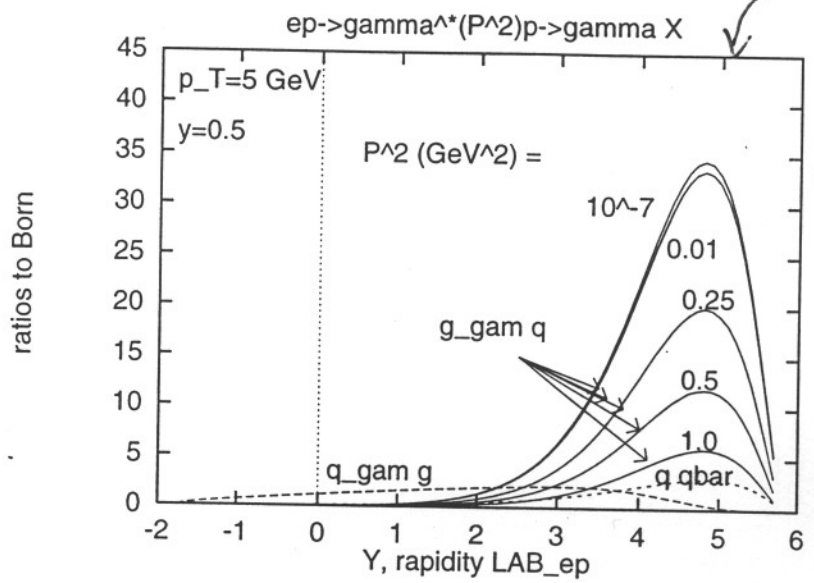

⇒ can we extract g^{γ^*}?

HERA

Figure 2. Ratios of the cross sections (see text) for the $ep \to e\gamma X$ with y=0.5 and p_T=5 GeV. The ratio to the Born cross section of the contributions due to $g^\gamma q^p \to \gamma q$ (solid lines) and $q^\gamma g^p \to \gamma q$ and $q^\gamma \bar{q}^p$ and $\bar{q}^\gamma q^p \to \gamma g$ (dashed lines) are presented for various values of the virtuality P^2 as a function of the Y. For the $g^\gamma q^p \to \gamma q$ results correspond to P^2=1 $\cdot 10^{-7}$, 0.01, 0.25, 0.5 and 1 GeV^2. For $q^\gamma g^p \to \gamma q$ and $q^\gamma \bar{q}^p$ and $\bar{q}^\gamma q^p \to \gamma g$ we take P^2= 0.1 GeV^2.

For THERA ratio $\dfrac{g^{\gamma^*} q^p \to \gamma q}{\gamma q^p \to \gamma q} = R$

eg. → $P^2 = 0.5\,\text{GeV}^2$ ...→ R = 300

(HERA --> R = 12)

$P^2 = 2\,\text{GeV}^2$ ...→ R = 10

↑ max

Hard virtual photon - proton collision

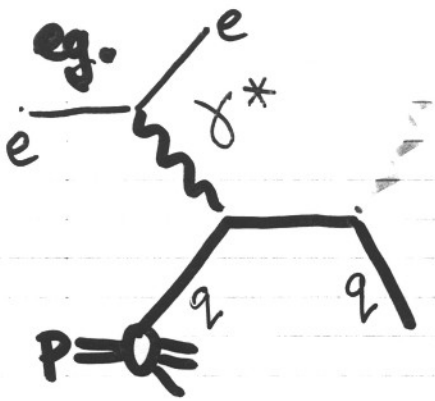

e.g. ↑ large p_T γ (prompt γ) + resolved γ* contribution

A. Zembrzuski MK '91; PRD57 '98

PHOTON 99 (hep-ph/9912368)

$p_T^2 \gg P^2 \gg \Lambda^2_{QCD}$ ← resolved γ*

(Q^2) So far only γ^*_T studied — γ^*_T contribution with GRS parton densities in γ^*_T

What about γ^*_L ?

Recent progress : (study of dijet production at HERA)

Effects of long. photons

- C. Friberg and T. Sjöstrand
  PHOTON 99 (hep-ph/9907245)
  hep-ph/0007314
  hep-ph/0009003

T. Gehrmann

- J. Chyla (+ M. Taševský)
  hep-ph/9912245
  hep-ph/0010055

parton (resolved) parametrization of γ^*_L

" The cont. of γ^*_L are substantial, particularly for small y, large P^2, low E_T and small x_γ "

Dijet production in $\gamma^* p$ (Chyla '2000) at HERA

γ^*_T vs γ^*_L

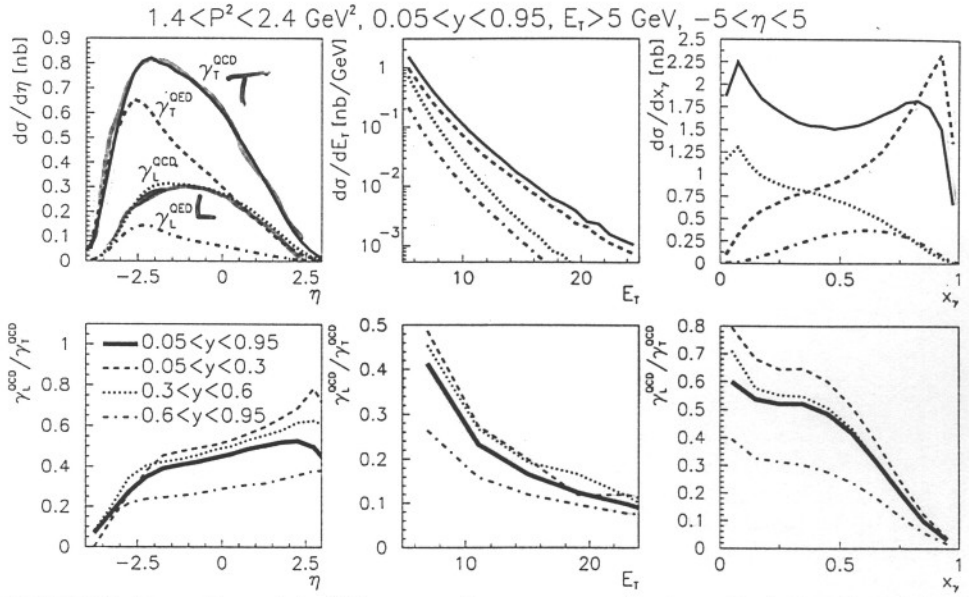

L/T

FIGURE 2. Upper three plots: dijet cross sections, corresponding to resolved γ^*_T and γ^*_L plotted as functions of η, E_T and x_γ for $1.4 \leq P^2 \leq 2.4$ GeV^2, $0.05 \leq y \leq 0.95$, $E_T \geq 5$ GeV, without any restriction on η. Lower three plots: the corresponding ratia of the contributions of γ^*_L and γ^*_T, integrated over the whole interval $0.05 \leq y \leq 0.95$, as well as in three indicated subintervals.

Hard virtual photon - proton collision

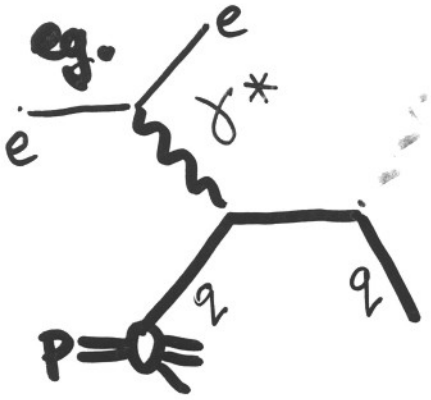

large p_T γ (prompt γ) + resolved γ^* contribution

A. Zembrzuski MK '91; PRD57 '98

PHOTON 99 (hep-ph/9912368)

$p_T^2 \gg P^2 \gg \Lambda^2_{QCD}$ ← resolved γ^*

(Q^2) So far only γ^*_T studied γ^*_T contribution with GRS parton densities in γ^*_T

What about γ^*_L ?

Recent progress: (study of dijet production at HERA)

Effects of long. photons

- C. Friberg and T. Sjöstrand
  PHOTON 99 (hep-ph/9907245)
  hep-ph/0007314
  hep-ph/0009003

- J. Chyla (+ M. Taševský)
  hep-ph/9912245
  hep-ph/0010055

parton (resolved) parametrization of γ^*_L

" The contr. of γ^*_L are substantial, particularly for small y, large P^2, low E_T and small x_γ "

Polarization states of virtual γ and separation of the transverse and longitudinal photon contributions in $\gamma^* p$ cross sections

V. Jezuita-Dąbrowska
MSc Thesis '99 ; and in preparation

$DIS_{ep}: ep \to eX$ (unpolarized case) one photon exchange

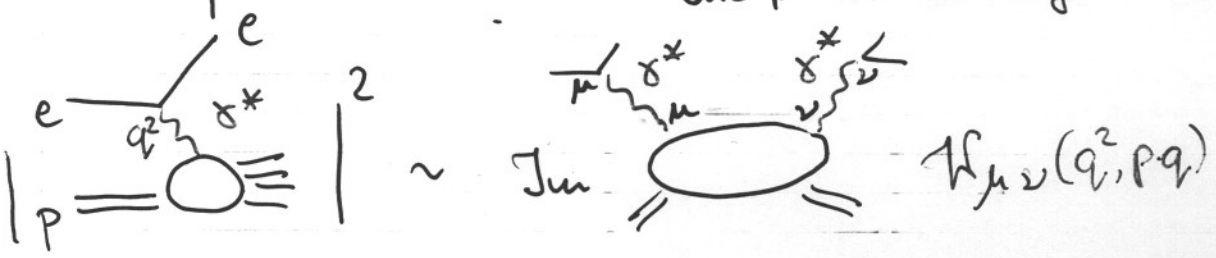

$$\sigma^{ep} \sim L^{\mu\nu} W_{\mu\nu} \sim \Gamma \left(\sigma_T^{\gamma^* p} + \varepsilon \sigma_L^{\gamma^* p} \right)$$

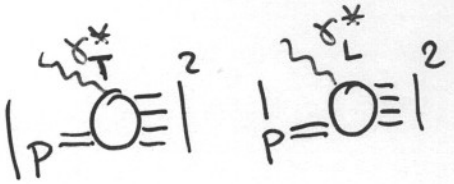

↑ factorization ↑ separation

The decomposition of propagator of γ^*

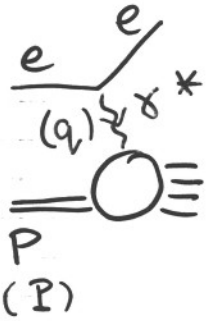

$$\leftarrow \quad \frac{-g^{\mu\nu}}{q^2} = \frac{\sum_\lambda \pm \varepsilon_\lambda^{*\mu}(q)\,\varepsilon_\lambda^{\nu}(q)}{q^2}$$

completness relation

$\lambda = 0,1,2,3$

ϵ^μ_λ - polarization vectors for γ^*

(in the Lorentz gauge $q\cdot\epsilon_\lambda = 0$)

for polarization vectors of the virtual photon in DIS we can take:

$$\varepsilon_3^\mu(q) = \frac{q^\mu}{\sqrt{|q^2|}}$$ ← due to gauge invariance this state is irrelevant for any observable $(q^\mu \mathcal{M}_{\mu\nu} = 0)$

$$\varepsilon_0^\mu(q,P) = \frac{P^\mu - \frac{P\cdot q}{q^2}q^\mu}{\sqrt{P^2 - \frac{(P\cdot q)^2}{q^2}}}$$ ← **laigitudinal pol.** ε_L^μ

$\varepsilon_0^\mu \cdot \varepsilon_{0,\mu} = +1$ (other name: scalar polar.)

$\varepsilon_1^\mu, \varepsilon_2^\mu$ ~ orthogonal to P^μ and q^μ

↑↑ **transverse pol.**

$$-g^{\mu\nu} + \frac{q^\mu q^\nu}{q^2} = \sum_{T=1,2} \varepsilon_T^\mu(q,P)\,\varepsilon_T^\nu(q,P) - \varepsilon_L^\mu(q,P)\,\varepsilon_L^\nu(q,P)$$

The propagator decomposition method can be used to factorize and separate cont's in $\sigma_{ep\to eX}$.

Can we use it to factorize and separate cross section for $ep \to e$ (large p_T particle) X ?

Take the process

$$ep \to e\gamma X$$

at the Born level :

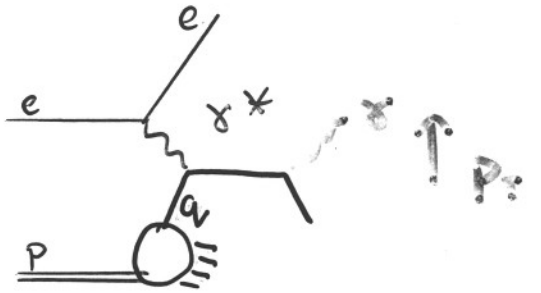

and check

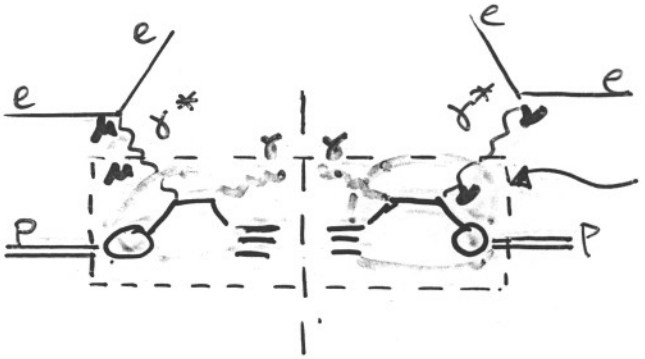

$T_{\mu\nu}(q^2, p\cdot q, p^2)$

Explicite forms of polarization vectors

⊙ linear polarization

$$T^{\mu\nu} \sim A\,\varepsilon_1^{*\mu}\varepsilon_1^{\nu} + B\,\varepsilon_2^{*\mu}\varepsilon_2^{\nu} + C\,\varepsilon_L^{*\mu}\varepsilon_L^{\nu} - D\,(\varepsilon_2^{*\mu}\varepsilon_L^{\nu} + \varepsilon_L^{*\mu}\varepsilon_2^{\nu})$$

← no separation!

⊙ circular polarization

$$T^{\mu\nu} \sim \tilde{A}\,(\varepsilon_+^{*\mu}\varepsilon_+^{\nu} + \varepsilon_-^{*\mu}\varepsilon_-^{\nu}) + \tilde{B}\,(\varepsilon_+^{*\mu}\varepsilon_-^{\nu} + \varepsilon_-^{*\mu}\varepsilon_+^{\nu}) + C\,\varepsilon_L^{*\mu}\varepsilon_L^{\nu} - \tilde{D}\,(\varepsilon_L^{*\mu}\varepsilon_+^{\nu} - \varepsilon_+^{*\mu}\varepsilon_0^{\nu} - \varepsilon_0^{*\mu}\varepsilon_-^{\nu} + \varepsilon_-^{*\mu}\varepsilon_L^{\nu})$$

← no separation

So, we have

σ_T, σ_L, τ_{TL} terms! $\tau_{TL} < 0$! $|\tau_{TL}| \sim \sigma_L$

$ep \to e\gamma X$ via γ^* exchange

Born level $Q^2 = 10\,GeV^2$

$P_T^\gamma = 5\,GeV$

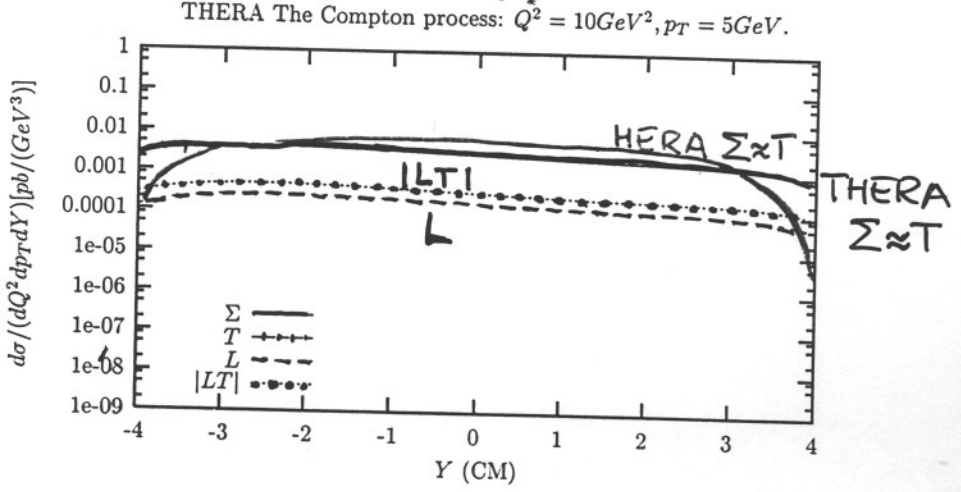

For $Q^2 = 0.1\,GeV^2$ $P_T = 2, 5, 20\,GeV$

1

10

100

so

$\Sigma \approx T$ since $(L - LT) \approx 0$

$\gamma^* \approx \gamma_T^*$

"L/T" ratio at Y=0

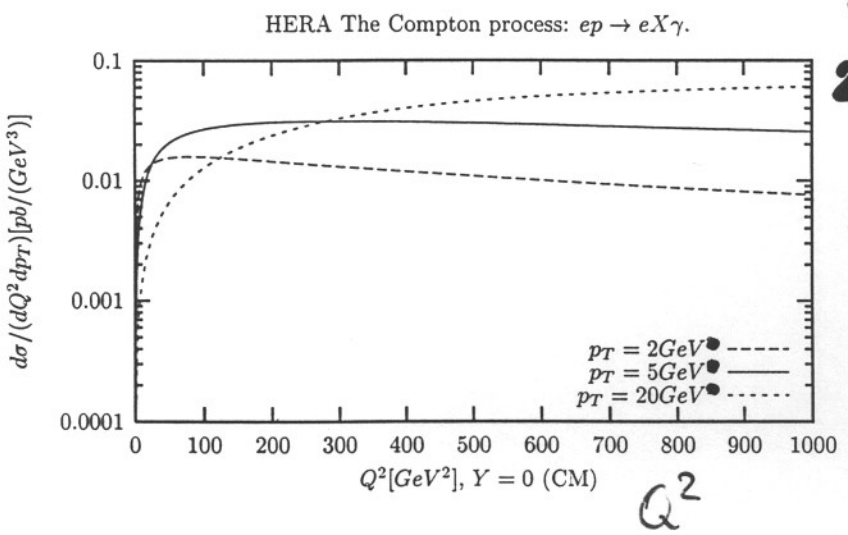

P_T = 20 5 2 GeV

Q^2

THERA ~ HERA

Conclusion:

In $ep \to e\gamma X$ with $p_T^{\gamma} \sim 2\text{-}20$ GeV

the diff. cross section (Born) has contributions

$$\sigma_T^{\gamma^* p}, \quad \sigma_L^{\gamma^* p} \quad \text{and} \quad \tau_{TL}^{\gamma^* p}$$

$\sigma_T^{\gamma^* p}$, $\sigma_L^{\gamma^* p}$ — they cancel each other

so $\sigma^{\gamma^* p}$ is given by $\sigma_T^{\gamma^* p}$ alone

How one can estimate the size of the resolved longitudinal γ^* cont'n in presence of $\tau_{TL}^{\gamma^* p}$ term?

Has the QCD RG-improved partan content of γ^* been observed?

M. Glück, E. Reya, I. Schienbein
hep-ph/0009348

e^+e^- and DIS$_{ep}$ data on structure of γ^*
⇝ standard 'naive' quark-parton model box approach describes data

⇝ thus, the QCD improved partonic densities of γ^*, in particular g^{γ^*}, have not yet been observed

⇝ future observation

$e^+e^- \to e^+e^- c\bar{c} X \quad \rightsquigarrow g^{\gamma(P^2)}$

charm cont. to F_2^γ for $x \lesssim 0.05$ will be sensitive to gluonic content of γ^*

$f^{\gamma(P^2)}(x, Q^2)$ at not too large x (≲0.3) and P^2 (≲5 GeV^2) from dijets (DIS$_{1r}$)

$\bar{Q} \equiv E_T \simeq 5-10$ GeV

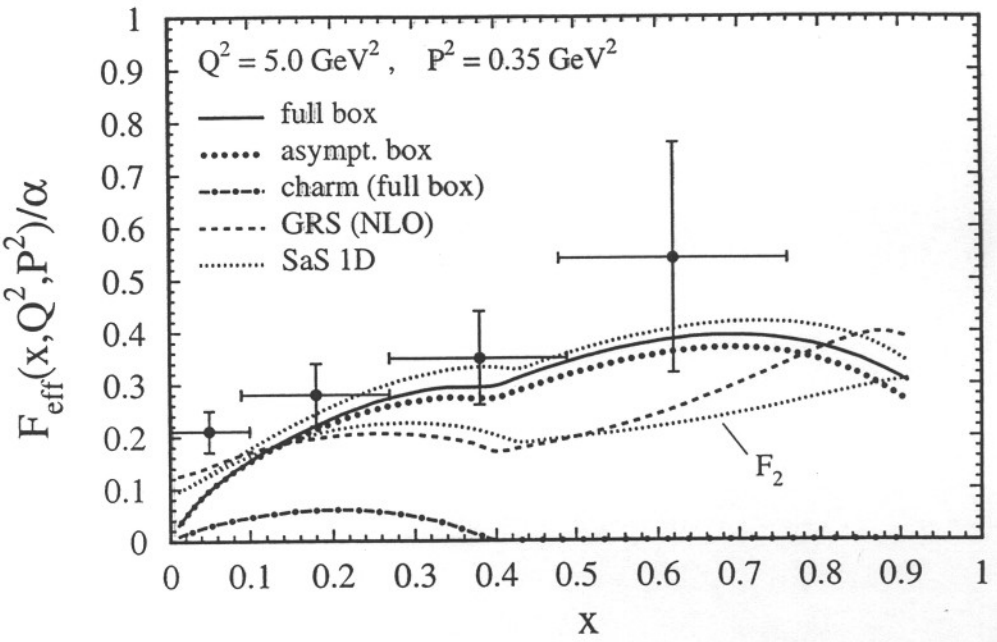
$Q^2 = 5.0\ GeV^2$, $P^2 = 0.35\ GeV^2$
full box
asympt. box
charm (full box)
GRS (NLO)
SaS 1D
F_2
$F_{eff}(x,Q^2,P^2)/\alpha$
x
0
0.1
0.2
0.3
0.4
0.5
0.6
0.7
0.8
0.9
1

Fig. 1

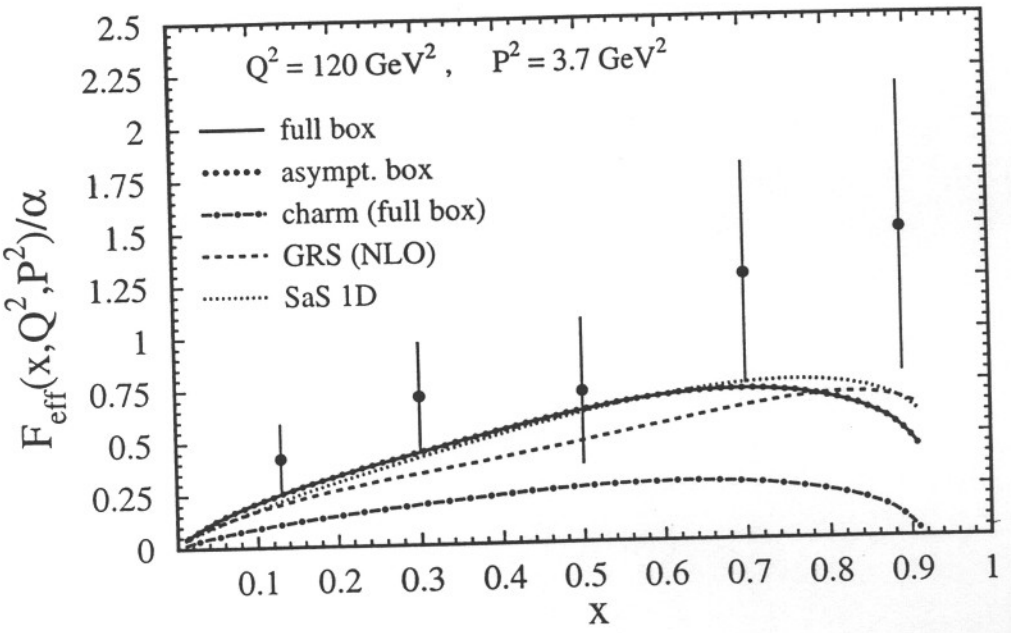
$Q^2 = 120\ GeV^2$, $P^2 = 3.7\ GeV^2$
full box
asympt. box
charm (full box)
GRS (NLO)
SaS 1D
$F_{eff}(x,Q^2,P^2)/\alpha$
x
2.5
2.25
2
1.75
1.5
1.25
1
0.75
0.5
0.25
0
0.1
0.2
0.3
0.4
0.5
0.6
0.7
0.8
0.9
1

Fig. 2

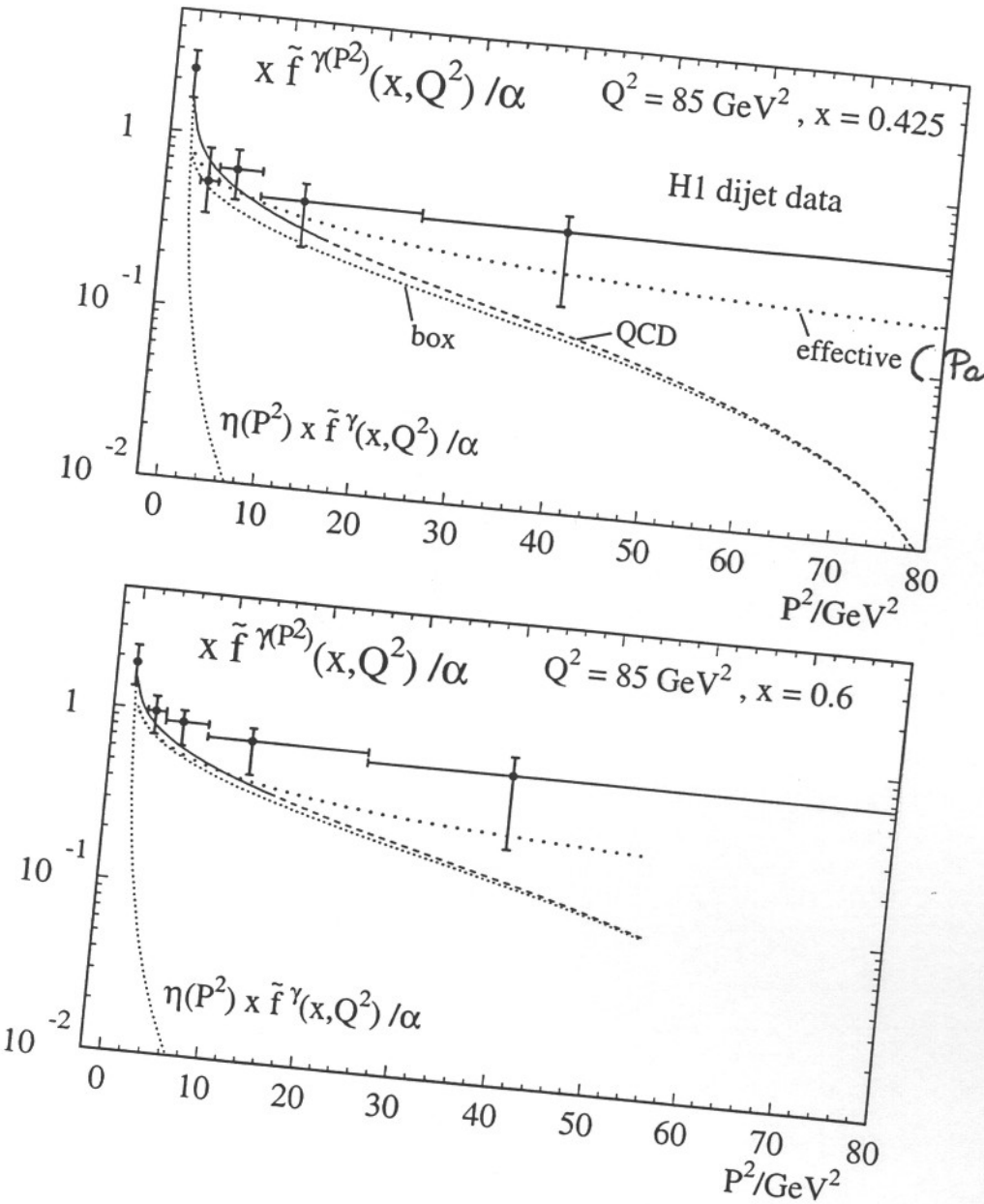
x f̃ γ(P2)(x,Q2) /α
Q2 = 85 GeV2 , x = 0.425
H1 dijet data
box
QCD
effective (Parton Model)
η(P2) x f̃ γ(x,Q2) /α
P2/GeV2
x f̃ γ(P2)(x,Q2) /α
Q2 = 85 GeV2 , x = 0.6
η(P2) x f̃ γ(x,Q2) /α
P2/GeV2

Fig. 3

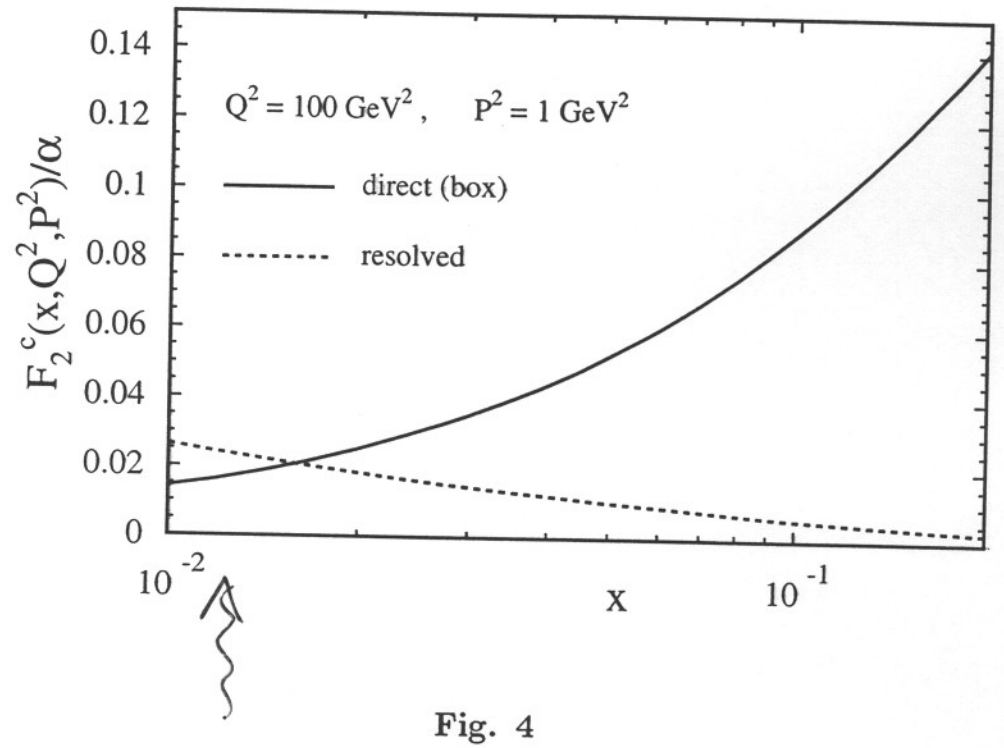
0.14
0.12
0.1
0.08
0.06
0.04
0.02
0
$F_2^c(x,Q^2,P^2)/\alpha$
$Q^2 = 100\ GeV^2$, $P^2 = 1\ GeV^2$
direct (box)
resolved
10^{-2}
x
10^{-1}

Fig. 4

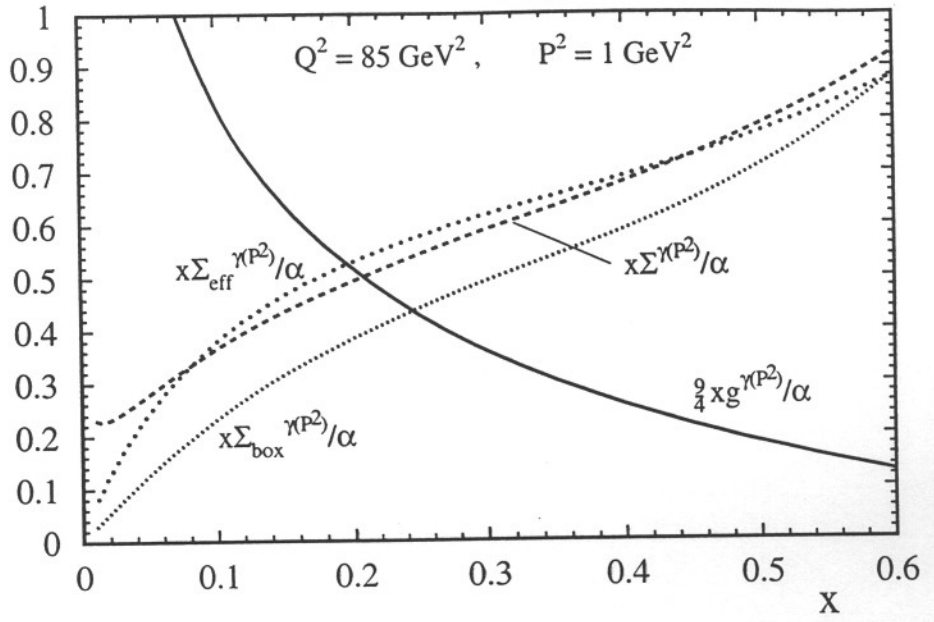
$Q^2 = 85\ GeV^2$, $P^2 = 1\ GeV^2$
$x\Sigma_{eff}^{\gamma(P^2)}/\alpha$
$x\Sigma^{\gamma(P^2)}/\alpha$
$\frac{9}{4}xg^{\gamma(P^2)}/\alpha$
$x\Sigma_{box}^{\gamma(P^2)}/\alpha$
X

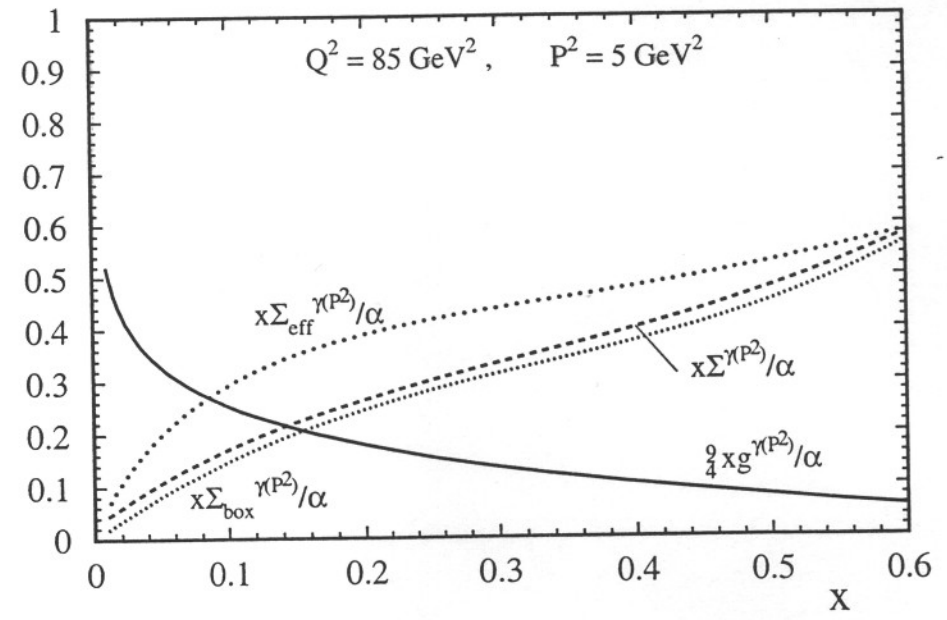
$Q^2 = 85\ GeV^2$, $P^2 = 5\ GeV^2$
$x\Sigma_{eff}^{\gamma(P^2)}/\alpha$
$x\Sigma^{\gamma(P^2)}/\alpha$
$\frac{9}{4}xg^{\gamma(P^2)}/\alpha$
$x\Sigma_{box}^{\gamma(P^2)}/\alpha$
X

Fig. 5

Resolved Photons at HERA and THERA

Boris Levchenko

INP Moscow State Univ.

Let consider NC interactions and denote the components of the incoming $e^{\pm}$ and p momenta as follows

$$\mathcal{K} = (\epsilon, 0, 0, -k), \quad \mathcal{P} = (E, 0, 0, P)$$

and mark the scattered particles with a prime.

A final state is characterized by a set of variables

$$k', \theta', P', \theta, x, y, Q^2, W, t \text{ etc.}$$

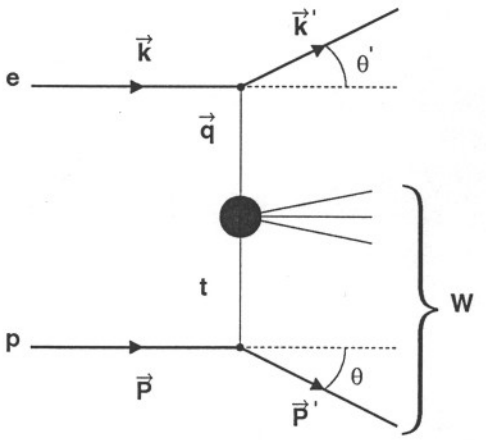

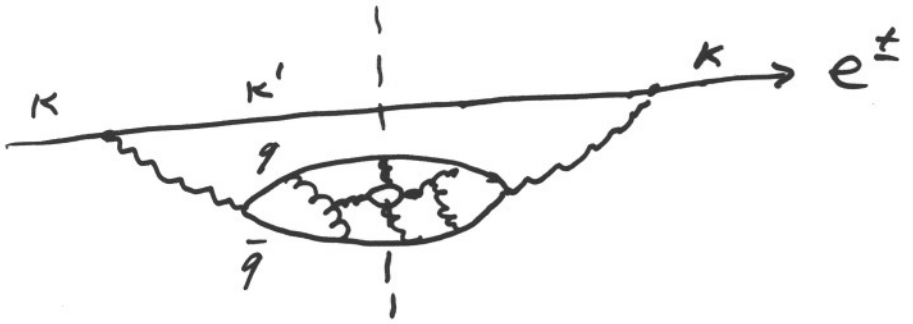

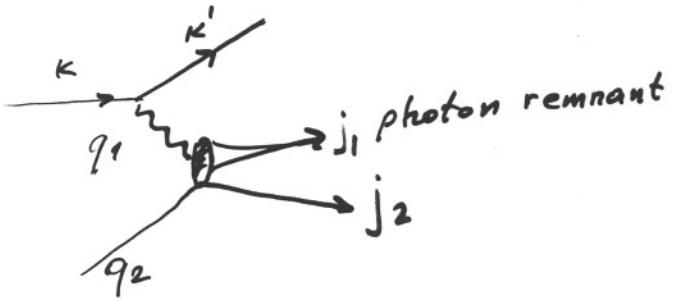

$$V(q_2) > V(q_1) = Q^2$$

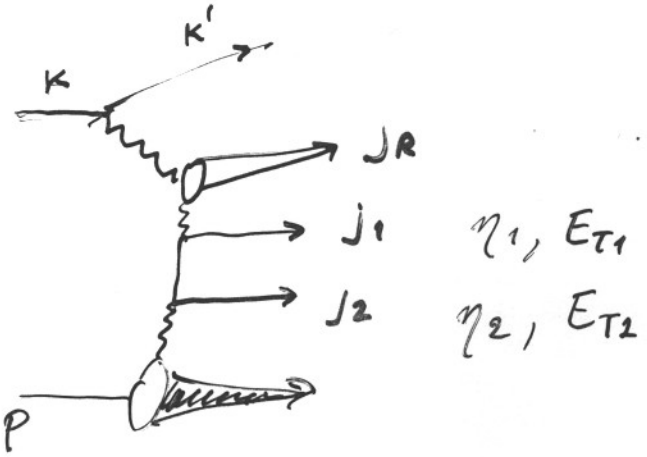

work in progress

Summary: inclusive

THERA - resolved γ

γ^*

processes

LC e^+e^- - F_2^γ, $F_2^{\gamma*}$

resolved $\gamma \propto \gamma^*$

processes

PC $e\gamma$ - F_2^γ!, resolved

$\gamma \propto \gamma^*$

$\gamma\gamma$ - resolved γ proces

Exclusive photoproduction

$\gamma p \to V p$ $\quad V = \rho, \omega, \varphi, J/\psi, \Upsilon$

Jim

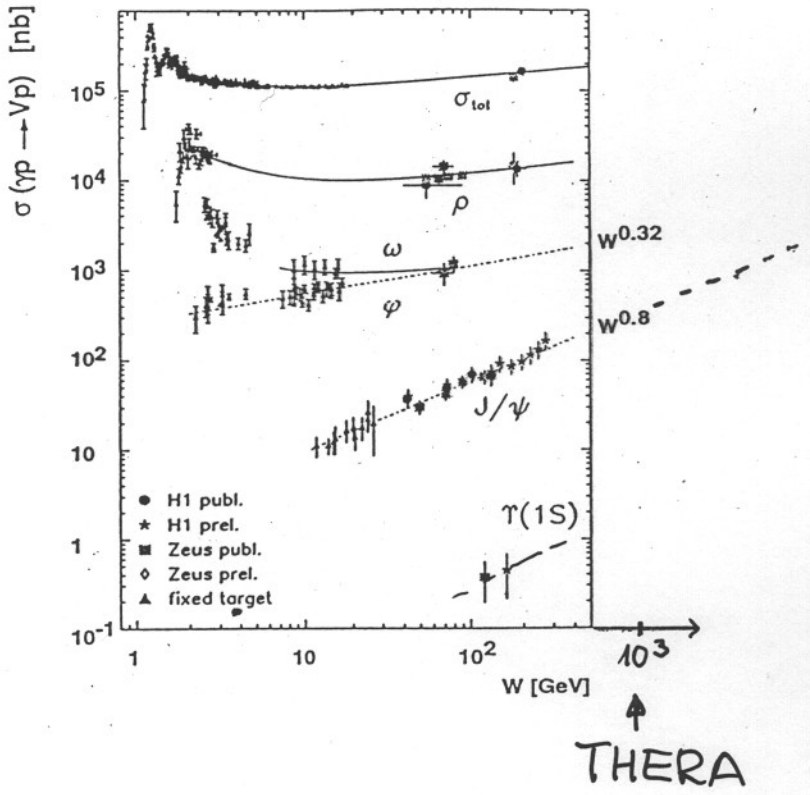

$\gamma p \to \pi^0 p$ $\quad \pi^0 \to \eta, \eta', \eta_c \ldots$ $\quad \to$ I. Ginzburg talk (April '2000)